Effect of Twisting on Mechanical Properties of GF/PP Commingled Hybrid Yarns and UD-Composites

A. R. Torun,[1] G. Hoffmann,[2] A. Mountasir,[2] Ch. Cherif[2]

[1]*Advanced Fibro-Science, Kyoto Institute of Technology, Matsugasaki 606-8585 Kyoto, Japan*
[2]*Institute of Textile Machinery and High Performance Material Technology, Technische Universität Dresden, 01062 Dresden, Germany*

Received 1 June 2010; accepted 4 March 2011
DOI 10.1002/app.34458
Published online 26 July 2011 in Wiley Online Library (wileyonlinelibrary.com).

ABSTRACT: This study was conducted due to the necessity for improving the processability of commingled yarns during textile processing, in particular dense 3D preform weaving. Open structure of the commingled yarns caused higher production stops. As a possible solution, GF/PP commingled yarns with different twisting levels were produced. Effect of twisting on the mechanical properties of commingled yarns and on their compression molded UD composites are determined. Further tests were executed about yarn/yarn and yarn/metal friction of twisted commingled yarns, which are important properties during textile processing. Theoretical approaches such as a yarn model with linear bar elements and lamina equation with an equivalent angle distortion of over-delivery proved useful to relate the structural parameters and mechanical properties. As a result, twisting did not significantly affect the modulus of elasticity of UD-composites, however, the tensile strength of UD-composites were reduced by further processing even without twisting. Therefore, small twisting levels can be applied on commingled yarns to improve processability of dense preforms without significantly affecting the mechanical performance. © 2011 Wiley Periodicals, Inc. J Appl Polym Sci 123: 246–256, 2012

Key words: composites; mechanical properties; processing; thermoplastics

INTRODUCTION

Thermoset polymers have been dominating the market as the matrix of choice for composites. Thermosets have lower viscosity in comparison with thermoplastics, which can be seen as the main advantage for the sake of processability. They also do not necessarily need pressure or heat during processing. Thermoset resins are generally inexpensive and stronger than thermoplastics with a higher serving temperature. Short workable pot life, the difficulties concerning the recycling issues and emission of volatile organic compounds are the main disadvantages. Thermoplastics offer higher impact strength and a good surface finish. They can be processed without emission of hazardous gases and recycled much easier.[1,2] Recycling is becoming more and more important due to the strict regulations of mass production industries, such as automobile industry.

The viscosities of fully polymerized thermoplastics are around two to three orders of magnitude higher than their thermoset counterparts.[3] To overcome the difficulties of impregnation caused by high viscosity of thermoplastics, reinforcement materials (e.g., carbon, glass) and thermoplastic polymer (e.g., PP, PEEK) are already mixed in solid state. The aim of solid state mixing is to reduce the flow path of polymers during impregnation. This mixture is processed into preforms mostly with textile machinery. Thermoplastic polymers in the preform are melted under the application of pressure and temperature (e.g., pultrusion, compression molding), and consolidated.[4–6]

Commingled yarns can be produced with a modified air-jet texturizing machine (Fig. 1). The most important modification is the type of air nozzle used. Commercial air nozzles are available, which claim to reduce the damage on the reinforcement yarns during processing and offer a better mixture in the crosssection. Especially for commingled yarns, a good mixture in the crosssection is crucial, because the main idea of commingling process is to reduce the flow paths of the viscous thermoplastic resin. Another important modification for commingling process is the bobbin winding device. Commingled yarns should be wound up with a constant yarn tension with higher bending radii of machine elements to minimize the damage on the yarn. Besides material mixing and high production rates, commingled yarns embody structural elongation which enables a

Correspondence to: A. R. Torun (refahtorun@gmail.com).
Contract grant sponsor: German Research Foundation

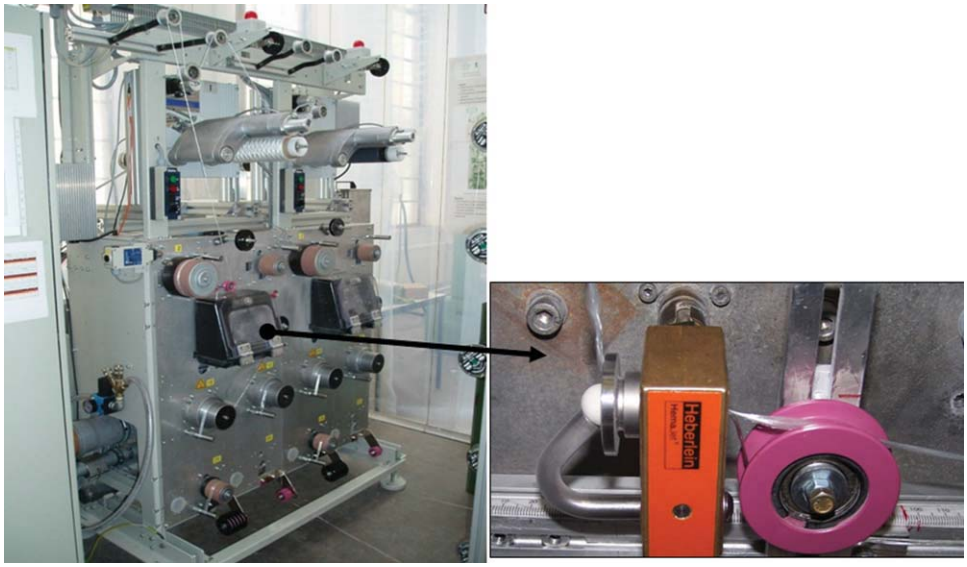

Figure 1 Air-jet texturizing machine utilized for commingled yarn production (left) and detail view of the air nozzle (right). [Color figure can be viewed in the online issue, which is available at wileyonlinelibrary.com.]

smoother processing with textile machinery. During commingling process, reinforcement yarns are damaged by the applied air pressure in the nozzle, which can be seen as a drawback. Another disadvantage of commingled yarns was identified from processing point of view while executing trials on high packing densities of 3D near-net shape woven preforms.[7–9] Harnesses apply forces on the warp yarns in both normal and longitudinal direction during weaving. These forces should be minimized by reducing the warp yarn tension especially for the brittle reinforcement yarns. However, reduced warp yarn tension with high packing density increases the probability of stuck yarns in the shed and causes unclear shed opening. After commingling, yarns become more voluminous and open. Depending on the structure, high packing density commingled yarns showed higher production stops than conventional materials, which necessitates improvement for the industrial production.

Over-delivery of input yarns is necessary for the formation of the commingled structure.[10] This indicates the possibility of slightly twisting the commingled yarn to create a more compact yarn structure without causing significant effect on the composite properties. In the literature, contributions about the effects of twisting on high performance yarns were reported however no study is available about the effect of twisting on the commingled yarns and their composites. Within the scope of this study, main aim is to determine whether twisting can be applied on commingled yarns to improve the processing behavior on textile machinery. The effect of twisting level both on the yarn and composite properties were analyzed to see how the physical and mechanical properties were changed. A yarn model with serially connected linear bar elements was introduced to consider the varying contribution of bulky and knot areas in the commingled yarn structure. Over-delivery of the constituent materials during commingled yarn production was modeled as an equivalent angle distortion of a lamia. Both yarn-yarn and metal-yarn friction areas occur during weaving. As the surface of the commingled yarn is altered through twisting, its effects on the friction coefficients between yarn-yarn and yarn-metal were analyzed.

EXPERIMENTAL

Materials

The GF/PP commingled yarns were produced with the commercial input materials of 300 tex glass (E 35, P-D Glasseiden GmbH, Germany) and 3 × 32 tex polypropylene (Prolen H, CHEMOSVIT FIBROCHEM a.s., Slovakia) which resulted in a fiber volume fraction of 52% in UD composites. Commingled yarns were produced with 4 bar air pressure in the nozzle and a winding speed of 100 m/min. To generate the commingled structure, input cylinders deliver the glass and polypropylene yarns with a higher speed than the output cylinder which is removing the final commingled yarn out of the air-nozzle. This setting is called over-delivery and defined as the percentage ratio of the speed difference to the output cylinder speed. Equation (1) shows the calculation of over-delivery OD, where S_i is the input speed of feeding cylinders and S_o is the output speed of take-up cylinders.

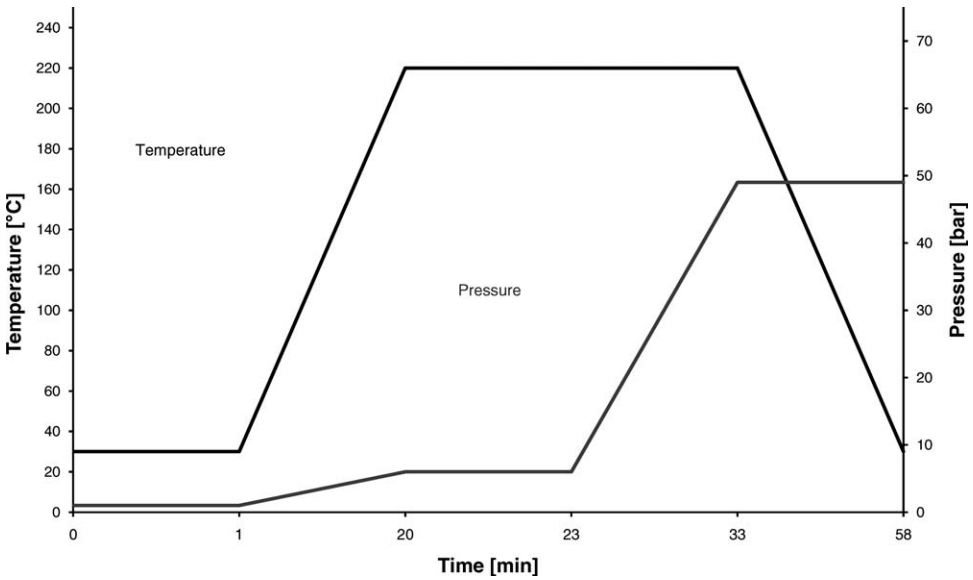

Figure 2 Processing parameters for compression molding of UD-composite plates.

$$\mathrm{OD} = \frac{S_i - S_o}{S_o} * 100 \quad (1)$$

Over-delivery of glass yarns was kept at a value of 2% to avoid damage and extensive loss of orientation. Over-delivery of polypropylene yarns was 8%, therefore polypropylene filaments had higher entanglement than glass filaments and were tending to be at the outer part in the cross section.

Produced commingled yarns were twisted (DirecTwist, Agteks) with 0, 5, 10, 15, 20, 40, and 60 tpm (twist per meter) and compared with the reference yarn which was commingled without any further process. 0 twist per meter in the trials actually means winding to another bobbin by using the same twisting machine. Winding without twist was done to isolate the effect of extra processing on the yarn properties. 5 to 20 tpm were the main experiments of concern, whereas 40 and 60 tpm experiments demonstrated extreme values. Unidirectional (UD) composites were produced with compression molding. Processing conditions for compression molding is shown in Figure 2.

Testing procedure

Yarn profiles as well as yarn–yarn and yarn–metal friction coefficients were determined by using dynamic tensile tester (LH-402 CTT-DTT Attachment, Lawson Hemphill). A CCD camera was used to measure the yarn diameter values with 3.25 micron precision when the yarn was moving at a speed of 100 m/min. Yarn–metal and yarn–yarn friction coefficients were determined dynamically according to ASTM D-3108, and ASTM D-3412. Tensile tests for yarns were executed with 20 specimens according to the norm DIN EN ISO 2062, with a clamping length of 500 mm and testing speed of 25 mm/min (Z100, Zwick GmbH and Co. KG). Tensile tests of UD-composites were executed according to DIN EN ISO 527-4. Upper and lower clamping areas were 50 mm each, and the testing lengths of the specimens were 150 mm. 0° specimens had a width of 15 mm and 90° specimens had a width of 25mm. 12 specimens for 0° and 8 specimens for 90° were tested for each twisting level and the reference. Testing speeds for both 0° and 90° were 2 mm/min. Confidence intervals with 95% were determined according to Student's *t*-distribution.

RESULTS AND DISCUSSION

Commingled yarn structure

Commingling process is based on the mixing of materials through an air nozzle. As in the air jet texturizing process, commingling process creates a special yarn structure with two different areas which are called as bulky and knot areas (Fig. 3). Continuous air pressure through the nozzle creates distinctive areas; in bulky region the materials are voluminous and open, whereas in knot areas they are intermingled together. Various process parameters such as nozzle type, air pressure, take-up speed, etc. affect the frequency and intermingling intensity of knot areas, however a fully control on this phenomenon is not possible. In the case of commingled yarns, a better mixture of reinforcement and matrix materials occurred in the knot area. Figure 3 demonstrates the cross sectional observations from bulky and knot areas, dark points are polypropylene and the light colored points are glass filaments.

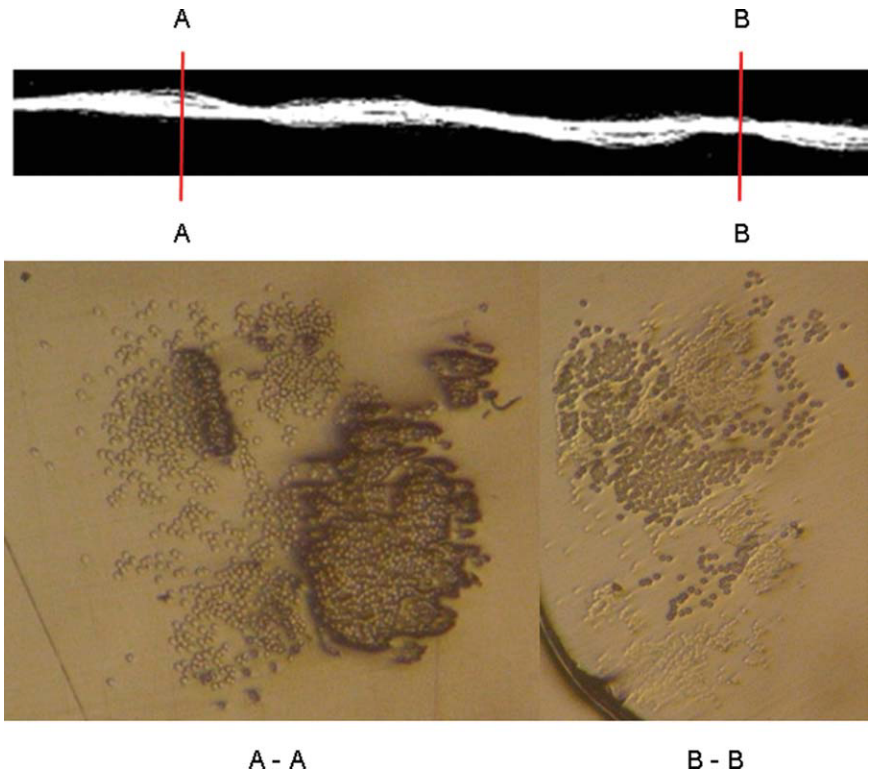

Figure 3 Cross-sectional observations of bulky (A-A) and knot (B-B) areas of GF/PP commingled yarns. [Color figure can be viewed in the online issue, which is available at wileyonlinelibrary.com.]

Profile scanning results demonstrated a progressive improvement of commingled yarn evenness with increasing A–A (Fig. 4). Bulky and B–B regions on commingled yarns were the main cause of production stops during weaving. The number of events, which is defined as ±50% variations in yarn diameter, was decreased from 42 events/m to the interval of 30–35 events/m for all twisting ratios.

Mean values of yarn diameter (Fig. 5) were increased for 0 tpm and 5 tpm samples, which was caused by the effect of the additional process step. After 10 tpm, yarn diameter decreased gradually. The standard deviation of every sample was less than the reference commingled yarn, thus more regular yarn structure was generated. Small yarn diameters enable denser packing of material during weaving. 3rd degree regression polynomial in Figure 3 has a local minimum around 55 tpm. After 60 tpm the diameter would not change significantly, however, the regression polynomial increases. Therefore the regression polynomial can be used for interpolation between the twisting values of 0 tpm and 60 tpm, but twisting values more than 60 tpm cannot be estimated with extrapolation.

Commingled yarn friction properties

In the literature the increase of friction coefficient for both yarn-to-yarn and yarn-to-metal with increasing twist values of multifilament yarns was reported.[11] Increasing twisting levels decreases the cross-sectional area and increases the hardness. The overall structure as well as the surface of commingled yarns are different than multifilament yarns. Twisting increases the surface roughness of a conventional mutifilament yarn. On the other hand, commingled yarns already have a high surface unevenness caused by the air-nozzle during production. Twisting increases the surface evenness of a commingled

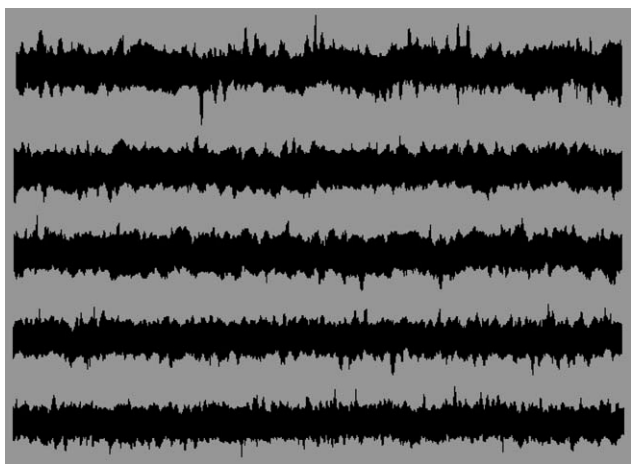

Figure 4 Comparison of GF/PP commingled yarn profile, from top to bottom; reference commingled yarn, 10tpm, 20tpm, 40tpm, 60tpm.

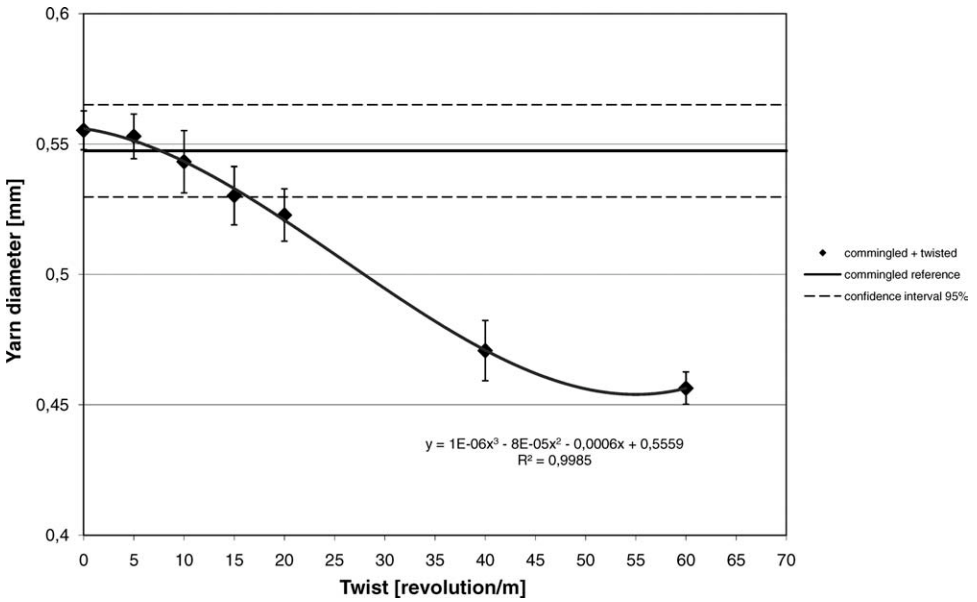

Figure 5 Effect of twisting on the diameter of GF/PP commingled yarns.

yarn which generates a tendency of decrease in coefficient of friction. Friction coefficient depends on the interaction of both touching surfaces. In the case of yarn-metal experiments, polished surface of the metal part suppressed the reduction tendency for the coefficient of friction. On the other hand, yarn–yarn friction had a linear decrease with increasing twist levels (Fig. 6). Yarn–metal friction coefficient increases with the increase of testing speed, so during weaving weft yarns yield around 20% higher friction coefficients than warp yarns.

Yarn mechanical properties

Figure 3 demonstrates the two different regions of commingled structure, therefore the modulus of elasticity was modeled with two linear bar elements (Fig. 7). This model aims to represent the varying contribution of the bulky and knot regions of commingled yarns on the tensile modulus. In the bulky region, voluminous structure is mainly created by the matrix material (PP), while reinforcing material (GF) remains straight. In the knot region, over-delivery of reinforcing material is consumed by the intensive intermingling. The two elements in Figure 7 represent the bulky area with straight reinforcement and the knot area with intermingled reinforcement yarns. The boundary of bulky and knot region cannot be always clearly defined. In addition, the intensity of intermingling in knot regions varies too.

The overall E-modulus was determined by the stiffness equation of serial springs [eq. (2)]

$$\frac{1}{k} = \frac{1}{k_1} + \frac{1}{k_2} \tag{2}$$

After putting the stiffness values of k_1 and k_2 into eq. (2), with the same cross-sectional areas A;

$$\frac{L_1 + L_2}{E^*A} = \frac{L_1}{E_1{}^*A} + \frac{L_2}{E_2{}^*A} \tag{3}$$

Rewriting eq. (3);

$$E = \frac{E_1{}^*E_2{}^*(L_1 + L_2)}{L_1{}^*E_2 + L_2{}^*E_1} \tag{4}$$

In the literature[12] a model was derived from laminate theory to determine the effect of twist on the E-modulus of some technical yarns such as Kevlar®, Vectran® etc. The model is in very good agreement with experimental data. Twisted yarn samples in those experiments should yield reduction of modulus which is caused by both the structural change by twisting and the yarn damage throughout processing. However, the damage on the yarns caused by twisting was not considered. Another previous study[13] predicted the relation between twisting angle and E-modulus of Nylon yarns with eq. (5). This equation progressively overestimated the E-modulus of technical yarns.[12] This slight overestimation compared with the experimental results is more reasonable to isolate only the effect of twisting without considering the yarn damage. Therefore, in this study eq. (5) was utilized to determine the reduction in modulus of elasticity caused by twisting.

$$\hat{E}(\alpha) = E_z{}^* \cos^2(\alpha) \tag{5}$$

Over-delivery of input materials in commingling process is necessary to create the knot areas, and

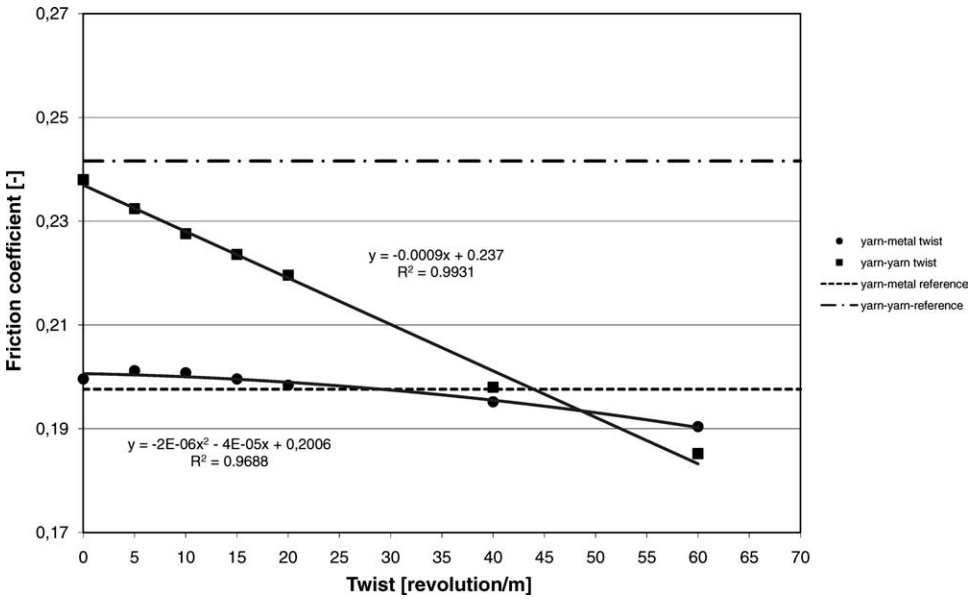

Figure 6 Effect of twisting on the yarn-yarn and yarn-metal friction of GF/PP commingled yarns.

most of the additional material length is integrated in these areas because the bulky region can easily be stretched during further processing. The twist angle equivalent of over-delivery ratio was calculated according to eq. (6), where α_{od} is twist angle equivalent caused by over-delivery and OD (%) is the over-delivery of input material.

Over-delivery of the reinforcement material within commingled hybrid yarn can be approximated as an angle distortion of a lamina. The input length of the reinforcement material is the hypotenuse of a right triangle and the output length is the adjacent side. Figure 8 demonstrates this approximation, where OD is the over-delivery as percentage and θ is the angle of distortion.

The inverse trigonometric function of cosine gives the equivalent of the distortion angle as shown in the eq. (6).

$$\alpha_{od} = \cos^{-1}\left(\frac{100}{100 + \mathrm{OD}}\right) \tag{6}$$

According to the assumption that the over-delivered material is mainly consumed in the knot areas, where the length is a ratio of overall yarn length, eq. (6) can be rewritten as;

$$\alpha_{od\_i} = \cos^{-1}\left(\frac{100 * \frac{L_i}{\sum_{j=1}^{n} L_j}}{100 * \frac{L_i}{\sum_{j=1}^{n} L_j} + \mathrm{OD}_i}\right) \tag{7}$$

Equation 7 is the general expression of how to distribute the angle distortion between n linear bar elements. The subscript i was used to distribute the overall over-delivery on the commingled yarn to the identified number of different regions. α_{od_i} stands for the angular distortion of the particular region and L_i is the representative length of that region. The summation symbol with L_j stands for the total representative length of the yarn. According to the model in Figure 7 there are two regions which represent the bulky and knot areas.

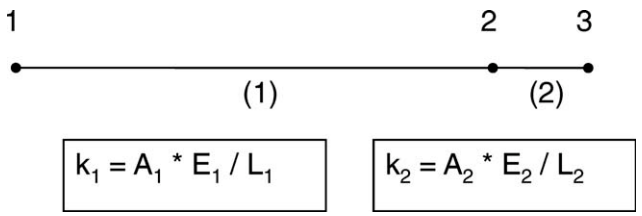

Figure 7 Model for determining the E-modulus of commingled yarns.

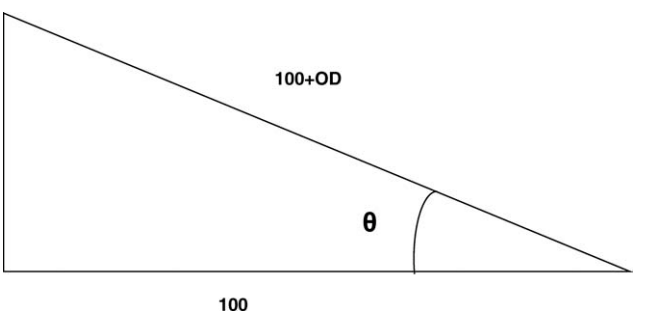

Figure 8 Schematic of equivalent angle distortion caused by over-delivery of reinforcing material.

Twist angle α_{tw} (degree) can be calculated according to the eq. (8), where d (mm) is the average yarn diameter and tw (tpm) is the twist value per meter.

$$\alpha_{tw} = \tan^{-1}\left(\frac{\pi^* d^* \mathrm{tw}}{1000}\right) \tag{8}$$

The total twist angle α_t is determined through superposition of the nominal twisting angle α_{tw} and the twist angle equivalent of over-delivery α_{od} as in eq. (9). After integrating eq. (9) into eq. (5), eq. (10) can be generated, which was used to calculate the modulus of elasticity of one element in Figure 5.

$$\alpha_t = \cos^{-1}\left(\frac{100 * \frac{L_i}{n}}{100 * \frac{L_i}{n} + \mathrm{OD}_i}\right) + \tan^{-1}\left(\frac{\pi^* d^* \mathrm{tw}}{1000}\right) \tag{9}$$

$$\hat{E}_i(\alpha) = E_i^* \cos^2\left(\cos^{-1}\left(\frac{100 * \frac{L_i}{n}}{100 * \frac{L_i}{n} + \mathrm{OD}_i}\right) + \tan^{-1}\left(\frac{\pi^* d^* \mathrm{tw}}{1000}\right)\right) \tag{10}$$

With the introduction of damage factor to the eq. (4) and the rule of mixtures the final equation for the determination of E-modulus becomes;

$$\hat{E}(\alpha) = D_r(\alpha_{tw}) * \frac{E_{r1}{}^* E_{r2}{}^* (L_1 + L_2)}{L_1{}^* E_{r2} + L_2{}^* E_{r1}} * Vf + \frac{E_{m1}{}^* E_{m2}{}^* (L_1 + L_2)}{L_1{}^* E_{m2} + L_2{}^* E_{m1}} * (1 - Vf) \tag{11}$$

Where E_{r1} is E-modulus of reinforcement element 1 (bulky region), E_{r2} is E-modulus of reinforcement element 2 (knot region), E_{m1} is E-modulus of matrix element 1 (bulky region), E_{m2} is E-modulus of reinforcement element 2 (knot region). All E-moduli are calculated with eq. (9). D_r is the damage factor which is a function of twist angle α_{tw} and multiplies only the reinforcement elements. Vf is the volume fraction of the reinforcing material.

Some simplifications and assumptions were done for the calculations. On the basis of the visual information, the length of the bulky region was approximately nine times the length of knot region which was reflected in the model with the length of elements. The reduction of E-modulus through twisting was mainly caused by the damage on the material because the orientation of the reinforcement material was not significantly affected within the trials. Over-delivery of glass yarns were 2%, in the calculations it is assumed that all this extra length is integrated into the knot area. Over-delivery of polypropylene was 8%, in the calculations it was assumed that the additional length was equally consumed in both bulky region and knot areas. An interesting phenomenon was the increase of both breaking force and E-modulus of commingled yarns after further processing. After twisting with 0° (only winding), yarn samples had higher E-modulus and breaking force than the reference yarn (Fig. 9). This is caused by the restructuring of the knot areas under tension, the yarn was stretched and the orientation of the reinforcement material in knot areas was increased. Figure 9 demonstrates the E-modulus and breaking force comparison of twisted and reference GF/PP commingled yarns. 40 tpm sample had almost same E-modulus and breaking force values as the reference sample. Reduction of E-modulus started with 60 tpm sample however the breaking force was still same as the reference yarn. These results indicate that the higher intermingling of filaments through twisting increases the mechanical properties of commingled yarns. Damage on glass fibers cannot be easily detected with yarn testing.

By using eqs. (10) and (11), theoretical E-modulus values were calculated for all the samples. Calculated theoretical E-modulus values were divided into 4 regions (Fig. 10) which were; measured E-modulus values during experiments as in Figure 9, loss of E-modulus caused by over-delivery during commingling [eq. (7)], loss of E-modulus caused by twisting [eq. (8)] and loss of E-modulus caused by the commingled process damage (difference between the theoretical E-modulus and the sum of the mentioned 3 regions). Although the y-axis presents the percentage of the regions within theoretical E-modulus values, the nominal E-modulus values (GPa) can be seen on the histograms. These results indicate that the commingling process reduces the yarn stiffness almost 50%. It is an important question whether the E-modulus reduction of commingled yarns affects the E-modulus of UD-composites in the same fashion.

UD composite properties

The 0° and 90° E-modulus calculations were executed according to laminate theory. Unlike the calculations for yarn E-modulus, UD-composite calculations were based on the homogeneous distribution of the glass filament in the PP matrix. Off-axis angle equivalent of over-delivery value for glass yarn was integrated to the equation, thus the UD composites structures were assumed to have a slight angle distortion.

Slab models deliver sufficient approximation to the elastic constants of a lamina. Within this model, aligned long fiber composites were treated as if the

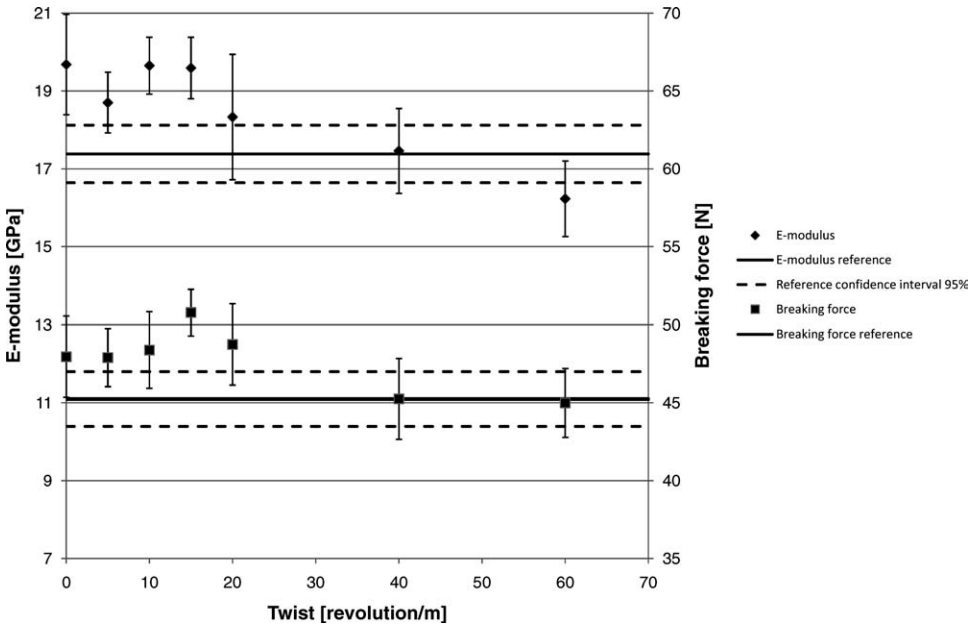

Figure 9 Effect of twisting on the E-modulus and breaking force of GF/PP commingled yarns.

two constituents of matrix and reinforcement are bonded together. Relative thicknesses of slabs were determined according to the volume fractions of fiber and matrix. Interface regions as well as local stress concentrations were ignored. E_1 (E-modulus fiber direction) is calculated according to equal strain assumption for both matrix and fiber in longitudinal direction. The eq. (12) is also called as "the rule of mixtures" and delivers a very good approximation. Discrepancies may results from the different poisson's ratios of matrix and reinforcement, however, it can be theoretically proved by the Eshelby model that the deviation is small under all conditions.[14,15]

$$E_1 = E_{1f}{}^{*}Vf + E_m{}^{*}(1 - Vf) \tag{12}$$

Transverse modulus of a composite with unidirectional fibers can also be approximated by a slab model which assumes an equal stress condition for matrix and fibers. The stress field is complex under transverse loading and in the literature, especially for thermoplastic matrices, underestimation of transverse modulus was reported. The modified equation

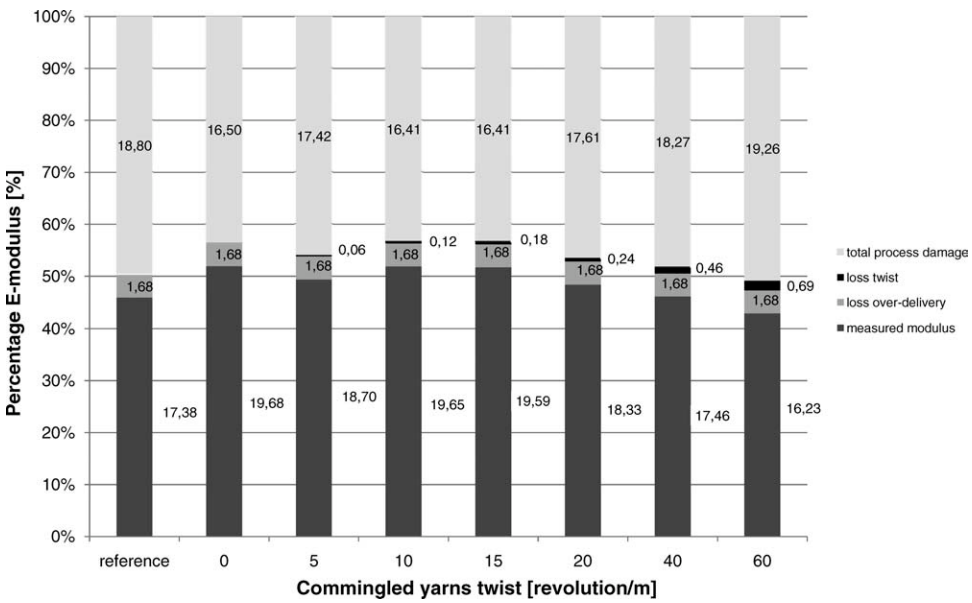

Figure 10 Distribution of E-modulus parts; difference between theoretical and measured modulus values.

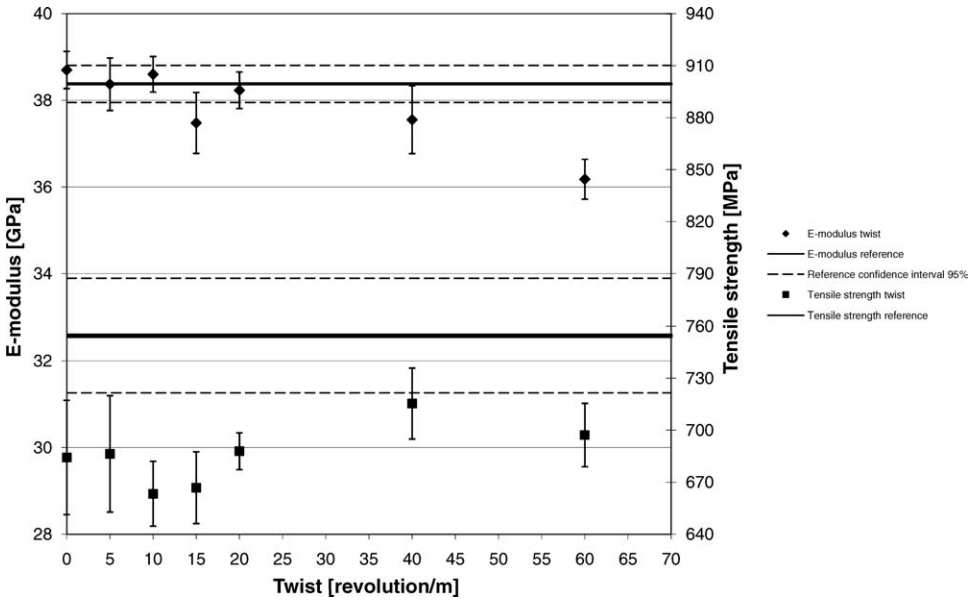

Figure 11 Modulus of elasticity and tensile strength of UD composites from GF/PP commingled yarns in 0°.

for the transverse modulus contains a correction factor η.[16–18] If η is taken as 1, the equation becomes the usual expression derived from an equal stress assumption for matrix and reinforcement. To fit the experimental data, η was taken as 0.6 which compensates the above-mentioned underestimation of transverse modulus.

$$E_2 = \frac{Vf + \eta^*(1 - Vf)}{\frac{Vf}{E_{2f}} + \frac{\eta^*(1 - Vf)}{E_m}} \tag{13}$$

The expression for the in-plane shear modulus is analogous to the expression of transverse modulus because it assumes equal shear stress on the matrix and fibers. To avoid the underestimation, η′ parameter with 0.6 is applied in the calculations.

$$G_{12} = \frac{Vf + \eta'^*(1 - Vf)}{\frac{Vf}{G_{12f}} + \frac{\eta'^*(1 - Vf)}{G_m}} \tag{14}$$

Since the equal strain assumption is applicable to a UD lamina, the poisson's ratio can be determined by "the rule of mixtures."

$$\nu_{12} = \nu_{12f}{}^* Vf + \nu_m{}^*(1 - Vf) \tag{15}$$

According to the above expression, 2% over-delivery of glass filaments was equivalent to 11.36° off-axis angle distortion. The off-axis longitudinal and transverse stiffness were calculated according to laminate theory. The relation between stress and strain tensors in the principal material direction is given in eq. (16).

$$\{\sigma\} = [\theta]\{\varepsilon\}$$

$$[Q] = \begin{bmatrix} Q_{11} & Q_{12} & 0 \\ Q_{12} & Q_{22} & 0 \\ 0 & 0 & Q_{66} \end{bmatrix}$$

$$Q_{11} = \frac{E_1}{1 - \frac{\nu_{12}^2 E_2}{E_1}}$$

$$Q_{12} = \frac{\nu_{12} E_2}{1 - \frac{\nu_{12}^2 E_2}{E_1}}$$

$$Q_{22} = \frac{E_2}{1 - \frac{\nu_{12}^2 E_2}{E_1}}$$

$$Q_{66} = G_{12} \tag{16}$$

The transformation of the stresses from principal material direction to an arbitrary coordinate system can be done with a modified reduced-stiffness matrix [Q'] as in eq. (16), where $m = \cos\theta$ and $n = \sin\theta$.

$$[Q'] = \begin{bmatrix} Q'_{11} & Q'_{12} & Q'_{16} \\ Q'_{12} & Q'_{22} & Q'_{26} \\ Q'_{16} & Q'_{26} & Q'_{66} \end{bmatrix}$$

$$\begin{aligned} Q'_{11} &= Q_{11}m^4 + Q_{22}n^4 + 2m^2n^2(Q_{12} + 2Q_{66}) \\ Q'_{12} &= m^2n^2(Q_{11} + Q_{22} - 4Q_{66}) + (m^4 + n^4)Q_{12} \\ Q'_{16} &= [Q_{11}m^2 - Q_{22}n^2 - (Q_{12} + 2Q_{66})(m^2 - n^2)]mn \\ Q'_{22} &= Q_{11}n^4 + Q_{22}m^4 + 2m^2n^2(Q_{12} + 2Q_{66}) \\ Q'_{26} &= [Q_{11}n^2 - Q_{22}m^2 + (Q_{12} + 2Q_{66})(m^2 - n^2)]mn \\ Q'_{66} &= (Q_{11} + Q_{22} - 2Q_{12})m^2n^2 + Q_{66}(m^2 - n^2)^2 \end{aligned} \tag{17}$$

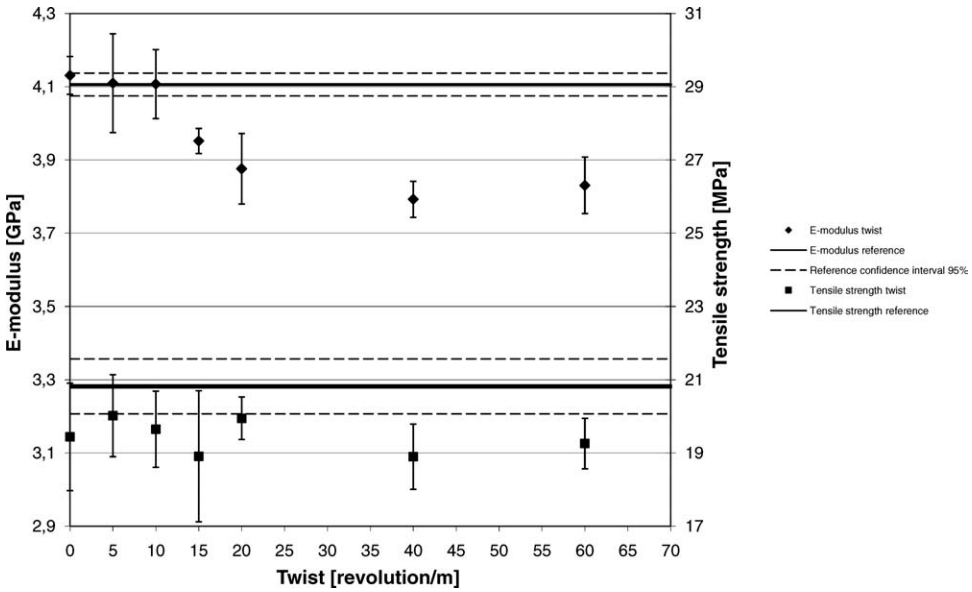

Figure 12 Modulus of elasticity and tensile strength of UD composites from GF/PP commingled yarns in 90°.

The modulus in the arbitrary x and y directions are defined as in eq. (18).

$$E_x = Q'_{11} - \frac{Q'^2_{12}}{Q'_{22}}$$
$$E_y = Q'_{22} - \frac{Q'^2_{12}}{Q'_{11}} \quad (18)$$

Stiffness value in longitudinal direction is found as 34.13 GPa which is underestimating the experimental results. Experimental results of longitudinal E-modulus in Figure 11 show agreement with the nominal values stiffness values according to the rule of mixtures. This indicates that the angle distortion caused by the over-delivery is disappeared during compression molding under tension. Modulus of elasticity in 0° direction is not much affected from twisting. Statistically, only the modulus of elasticity of the 60 tpm sample can be regarded as a reduction. On the other hand, the effect of further processing can be easily seen from the tensile strength reduction starting immediately with 0 tpm sample. All the samples had an overall tendency of strength reduction, however, between 0 tpm and 60 tpm samples, it cannot be concluded that higher twist reduces the strength more than lower twist.

Lamina stiffness calculation in transverse direction, 3.98 GPa, is in good agreement with overall experimental results (Fig. 12). It can be seen in Figure 5 that the yarn diameter is decreasing after 10 tpm. As the UD performs were prepared with the same amount of material, increasing compactness of the reinforcement material leads to greater resin rich areas. This reduces the E-modulus in transverse direction. Transverse tensile strength shows a slight reduction tendency with increasing twist level.

CONCLUSIONS

Effects of twisting on the mechanical properties of GF/PP commingled yarns are analyzed. This study is initiated through the production stops caused by the open and sticky commingled yarn structure during weaving of dense 3D woven preforms. A decreasing tendency of the yarn friction coefficient is observed unlike the results of other studies in the literature. The decrease is almost linear for yarn-yarn friction. Twisting decreases the average yarn diameter and creates a more compact and even structure. In commingled yarns, two distinctive areas can be recognized. These areas have varying mixing quality and yarn consumption. Increase of both E-modulus and tensile strength of commingled yarns are observed until 40tpm. A model is presented to calculate the yarn distortion effects on the E-modulus for over-delivery and twisting. Most of the E-modulus reduction can be explained with the damage on the material and structure change. The differences between the theoretical and calculated values were not observed in the UD-experiments. Longitudinal UD E-modulus values lay close to the theoretical values. A statistically confident reduction was observed after 40 tpm. However, UD tensile strength values of twisted samples were around 10% less than the reference commingled yarn. E-module in transverse direction starts decreasing with 20 tpm which correlates with the reduction in yarn diameter. A slight decrease in transverse tensile strength

was observed. Twist application on commingled yarns creates more compact yarn structure which can increase productivity in dense woven preform manufacturing. Up to 20 tpm twist levels can be applied where a longitudinal strength reduction of about 10% can be tolerated without any E-modulus reduction.

The authors express their sincere gratitude to German Research Foundation for the financial support of the collaborative research activities SFB 639. The fruitful cooperation with The Leibniz-Institut für Polymerforschung Dresden e. V. as well as NV Michel Van de Wiele Carpet and Velvet Weaving Machines are highly appreciated.

References

1. Aström, B. T. Manufacturing of Polymer Composites; Nelson Thornes Ltd: Cheltenham, 2002.
2. Flemming, M.; Ziegmann, G.; Roth, S.; Faserverbundweisen: Halbzeuge und Bauweisen; Springer Verlag: Berlin, 1997.
3. Advani, S. G.; Sozer, E. M. Process Modeling in Composite Manufacturing; Marcel Dekker: New York; 2003.
4. Offermann, P.; Wulfhorst, B.; Mäder, E. Technische Textilien/Technical Textiles 1995, 38, 55.
5. Bernet, N.; Michaud, V.; Bourban, P.-E.; Manson, J –A. E. Composites Part A 2001, 32, 1613.
6. Bourban, P.-E.; Bernet, N.; Znaetto, J.-E.; Manson, J-A E Composites Part A 2001, 32, 1045.
7. Torun, A. R.; Erdem, V.; Hoffmann, G.; Cherif, Ch. Technische Textilien/Technical Textiles 2009, 52, 142–144, E137–E139.
8. Torun, A. R.; Mountasir, A.; Hoffmann, G.; Cherif, Ch. JCCM-1; Kyoto, Japan, 2010.
9. Torun, A. R.; Hoffmann, G.; Cherif, Ch. 9th Texcomp: Delaware, USA 2008.
10. Choi, B.-D. Entwicklung von Commingling-Hybridgarnen für langfaserverstärkte thermoplastische Verbundwerkstoffe, Dissertation, Technische Universitaet Dresden, 2005.
11. Subramaniam, V.; Natarajan, K. S. Text Res J 1990, 60, 234.
12. Rao, Y.; Farris, R. J. J Appl Polym Sci 2000, 77 1938.
13. Hadley, D. W.; Pinnock, P. R.; Ward, I. M. J Mater Sci 1969, 4, 152.
14. Eshelby, J. D. Proc Roy Soc 1957, A241, 376–396.
15. Eshelby, J. D. Proc Roy Soc 1959, A252, 561–569.
16. Hyer, M. W. Stress Analysis of Fiber-Reinforced Composite Materials; McGraw-Hill, 1998.
17. Hull, D.; Clyne, T. W. An Introduction to Composite Materials; Cambridge University Press: Cambridge, 1996.
18. Halpin, J. C.; Tsai, S. W. Air Force Materials Laboratory Technical Report 1967, AFML-TR-67, 423.